Archives of Materials Science and Engineering

Volume 29
Issue 2
February 2008
Pages 73-80

International Scientific Journal
published monthly by the
World Academy of Materials
and Manufacturing Engineering

Correlation between fracture morphology and mechanical properties of NANOPERM alloys

S. Lesz [a,*], D. Szewieczek [b], J. Tyrlik-Held [c]

[a] Division of Nanocrystalline and Functional Materials and Sustainable Pro-ecological Technologies,Institute of Engineering Materials and Biomaterials, Silesian University of Technology, ul. Konarskiego 18a, 44-100 Gliwice, Poland
[b] Division of Materials Processing Technology, Management and Computer Techniques in Materials Science, Institute of Engineering Materials and Biomaterials, Silesian University of Technology, ul. Konarskiego 18a, 44-100 Gliwice, Poland
[c] Division of Biomedical Engineering, Institute of Engineering Materials and Biomaterials, Silesian University of Technology, ul. Konarskiego 18a, 44-100 Gliwice, Poland
* Corresponding author: E-mail address: sabina.lesz@polsl.pl

Received 12.12.2007; published in revised form 01.02.2008

ABSTRACT

Purpose: The purpose of this paper is to present of influence of heat treatment on the changes of structure, ductility, mechanical properties and particularly fracture morphology of the amorphous NANOPERM ribbons. The alloy was obtained in ribbons form by melt spinning method.

Design/methodology/approach: The following experimental techniques were used: scanning electron microscopy (SEM) and X-ray diffraction (XRD) phase analysis method to test the structure. The measurement of mechanical properties, like: tensile strength Rm, ductility ε were made. Tensile tests were performed on testing machine INSTRON 1195. Plastic properties of investigated ribbons were determined in bending test.

Findings: Morphology of fractures obtained after decohesion process in tensile test shows the history of amorphous alloys crystallization.

Practical implications: The relationship between heat treatments parameters, structure and mechanical properties can be useful for practical application of these alloys.

Originality/value: The temperature ranges of structure and mechanical properties changes after heat treatment of NANOPERM alloys it has been determined.

Keywords: Amorphous materials; Heat treatment; Mechanical properties; SEM; Fracture morphology; XRD method

MATERIALS

1. Introduction

As a result of research to date, two families of Fe-based alloys show the best performance characteristics and have emerged as the leading candidates for reduction to application: the FINEMET (Cu-Nb-B-Si) and the NANOPERM (Fe-M-B, where M=Nb, Hf, Zr).

The NANOPERM alloys are especially interesting because of their unique magnetic, mechanical and kinetic properties even in comparison with currently popular alloys such as FINEMET [1,2].

The FINEMET family is characterized by an optimum grain size of about 15 nm, provides a saturation induction of about 1.2

T, and exhibits very good properties at high frequencies. On the other hand, the grain sizes consistent with optimum performance are larger, around about 25 nm, in the NANOPERM family. The distinguishing feature of the NANOPERM family of alloys is the very low energy loss exhibited at low frequencies [1-6].

Rapid solidification using melt spinning is the technique employed to prepare the precursor amorphous alloys. The nanocrystalline materials are obtained by crystallizing precursors cast as amorphous alloy ribbons. The amorphous alloys typically crystallize in two stages: a magnetically desirable bcc-(Fe, X) phase appears first, followed by a boride phase, the presence of which is deleterious to good soft magnetic properties. In the optimized chemistries, the separation between the two crystallization events is large (≅150 K), so that crystallizing heat treatments may be conducted above the temperature for the first event, while safely avoiding the onset of the other [3,7].

Bcc α-Fe nanocrystallites embedded in amorphous matrix can be produced by an annealing treatment, during which amorphous alloys are annealed at different temperatures above their crystallization temperatures [3,7,8]. The process of crystallization is the nucleation of embryos that are crystallization centers. The second process is the growth of crystals from these centers. The crystallization process is determined by two factors: the nucleation rate and the crystal growth rate [3,8]

Well known as the most effective influence on nanocrysatallization is Nb addition. Thanks to its low diffusion coefficient the process of α-Fe grains growth is slowing down. Increase of Nb content causes the shift of crystallization stages to higher temperature, as well makes differences between crystallization stages bigger. Cu addition multiply the number of nucleation places especially during primary crystallization. Crystallization process results on changes as well physical as mechanical properties [9-15].

Nanocrystalline soft magnetic alloys such as NANOPERM have attracted a great deal of attention over the past 10 years. The influence of heat treatment on the magnetic properties of NANOPERM alloys is the most extensively studied [1,2,5-8,11,14,15]. However, there are only few papers on the influence of heat treatment on the fracture morphology and mechanical properties of ribbons, especially their brittleness/ductility [9,10, 12,13]. The brittleness is a limiting factor for many technological applications of soft magnetic materials. Hence, in the present paper investigations of changes of fracture morphology and mechanical properties, (especially tensile strength R_m, and ductility ε) involved by heat treatment of amorphous NANOPERM ribbons of different chemical composition compared to as-quenched state has been undertaken.

2. Experiments

Investigations were carried out on amorphous NANOPERM ribbons of $Fe_{85.4}Hf_{1.4}B_{13.2}$ (Fe-85.4, Hf-1.4, B-13.2 %at.), $Fe_{76.6}Hf_{6.4}B_{17}$ (Fe-76.6, Hf-6.4, B-17.0 %at.) and $Fe_{84}Nb_7B_9$ (Fe-84.0, Nb-7.0, B-9.0 %at). The ribbons of $Fe_{85.4}Hf_{1.4}B_{13.2}$, $Fe_{76.6}Hf_{6.4}B_{17}$, $Fe_{84}Nb_7B_9$ alloy had 0.024, 0.020, 0.037 mm thickness and 10.0, 8.0, 5.0 mm width, respectively. Amorphous NANOPERM ribbons has been prepared by planar flow casting method from the melt.

Depending on chemical alloy composition different parameters of annealing temperature have been used. The samples of the Fe-Hf-B and Fe-Nb-B ribbons were annealed in temperature range of T_a=373-1023 K and T_a=573-973 K, respectively. Annealing time for all alloys was the same and equal to 1 h.

The microstructure of the ribbons was examined by X-ray diffraction (XRD) and SEM method.

The changes of ribbons structures involved by heat treatment have been investigated by X-ray method. X-ray diffraction phase analysis has been performed by the use of diffractometer DRON 2.0 and XRD 7, SEIFERT-FPM firm with filtered Co-Kα radiation.

Tensile tests were performed on testing machine INSTRON 1195 with tension rate 5 mm/min. Plastic properties of investigated ribbons were determined in bending test which is the method generally used for amorphous tapes. Ribbons were bended of 180° angle, and then the value of ε was determined by used Eq 1:

$$\varepsilon=2g/h \quad (1)$$

where: g - sample thickness; h - distance between micrometer jaws in the moment of appearing the fracture.

There were prepared 5 samples on each state for carrying out the mechanical properties investigations. The results have been worked out with the use of statistic methods.

The morphology of fracture surfaces after decohesion in tensile tests was observed in scanning electron microscope OPTON DSM 940.

The observed changes of structure and properties were compared with as quenched alloys.

3. Results and discussion

It was found from the obtained results of structural studies of amorphous NANOPERM alloys that heat treatment involved changes of phase composition, which are corresponding with characteristic differences in fracture morphology and mechanical properties, comparing with amorphous state. The annealing temperature ranges T_a relating to structural relaxation, primary and second crystallization as well as mechanical properties (ε, R_m) of investigated alloys have been presented in the Table 1-3.

All investigated alloys had amorphous structure in as quenched state. Tensile strength R_m of $Fe_{85.4}Hf_{1.4}B_{13.2}$, $Fe_{76.6}Hf_{6.4}B_{17}$, $Fe_{84}Nb_7B_9$ alloys was equal to 237, 179, 732 MPa, respectively. Ductility of all alloys was high (ε=1) (Table 1-3).

Investigations of the fractures after decohesion in tensile test confirmed high plasticity of ribbons and revealed their ductile character with vein pattern morphology, typical for amorphous alloys (Figs. 1-3).

Proceeding of the changes of structure, mechanical properties, ductility and fracture morphology after decohesion in tensile testing in investigated alloys, involved by heat treatment has different character.

Annealing of the $Fe_{85.4}Hf_{1.4}B_{13.2}$ alloy at temperature below 523 K didn't involve the changes of structure and plastic properties of the samples in compare to as quenched state. A typical vein pattern morphology has been still seen (Fig. 4). Tensile strength R_m vary between 560 and 197 MPa (Table 1).

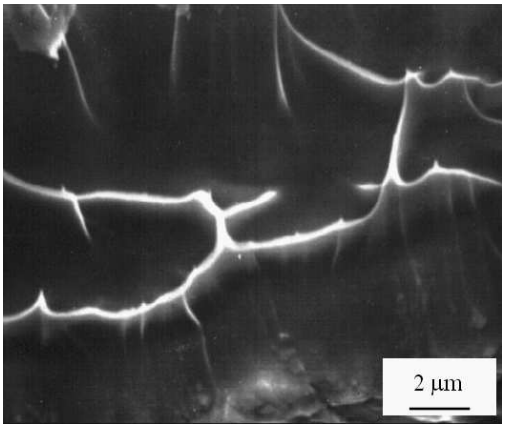

Fig. 1. SEM image of fracture surface of $Fe_{85.4}Hf_{1.4}B_{13.2}$ ribbons after decohesion in tensile test - as quenched state; vein pattern morphology

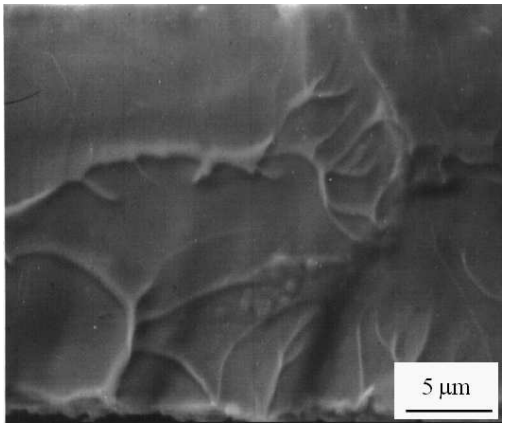

Fig. 2. SEM image of fracture surface of $Fe_{76.6}Hf_{6.4}B_{17}$ ribbons after decohesion in tensile test - as quenched state; vein pattern morphology

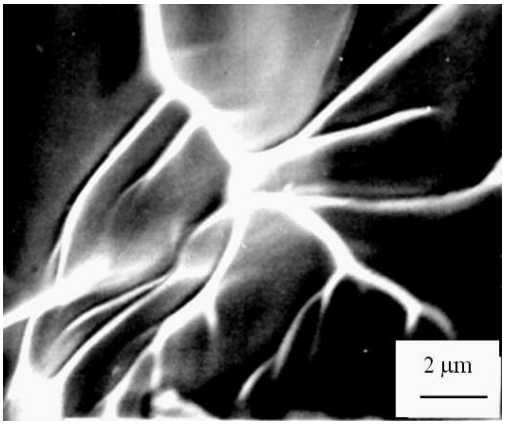

Fig. 3. SEM image of fracture surface of $Fe_{84}Nb_7B_9$ ribbons after decohesion in tensile test - as quenched state; vein pattern morphology

Heat treatment process in temperature range from 523 K up to 573 K leads to crystallization of amorphous $Fe_{85.4}Hf_{1.4}B_{13.2}$ alloy. As a result of the primary crystallization in structure of ribbons annealed in temperature range 523-573 K, coexistence of amorphous phase and αFe phase has been stated (Table 1).

Table 1.
Influence of heat treatment on phase composition and mechanical properties (R_m, ε) of amorphous $Fe_{85.4}Hf_{1.4}B_{13.2}$ alloy

Heat treatment parameters		Phase composition	Tensile strength	Plastic deformation
Temperature T_a [K]	Time [h]		R_m [MPa]	ε
as quenched	1		237	1
373	1		560	1
423	1	A	536	1
473	1	(S.R.)	249	1
498	1		197	1
523	1	A+αFe	345	1
573	1	(P.C.)	307	1
623	1		108	0.043
673	1		96	0.023
723	1	αFe,	16	0.025
773	1	Fe_2B,	8	0.009
823	1	HfB_2,	5	0.008
873	1	FeB,	4	0.010
923	1	Fe_2Hf	*	0.011
973	1	(S.C.)	*	0.017
1023	1		*	0.019
A – amorphous phase, (S.R.) – structural relaxation				
(P.C.) – primary crystallization, (S.C.) – second crystallization				
* - because of high brittleness of ribbons annealed from 923 K tensile tests haven't been carried out				

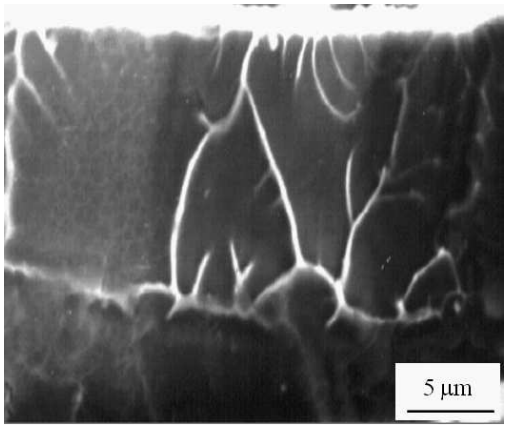

Fig. 4. SEM image of fracture surface of $Fe_{85.4}Hf_{1.4}B_{13.2}$ ribbons after decohesion in tensile test - annealing temperature 423 K/1h; ductile vein pattern morphology

Ribbons annealed in the above temperature range have still high ductility (ε=1) (Table 1) and high tensile strength R_m varied between 345 and 307 MPa (Table 1). In temperature range of

523-573 K the first changes in fracture morphology compare to amorphous state have been stated. A vein pattern morphology has been still seen (Figs. 5,7) but large areas of chevron pattern morphology on the failure surface has been observed too (Figs. 6,8).

Table 2.
Influence of heat treatment on phase composition and mechanical properties (R_m, ε) of $Fe_{76.6}Hf_{6.4}B_{17}$ amorphous alloy

Heat treatment parameters		Phase composition	Tensile strength	Plastic deformation
Temperature T_a [K]	Time [h]		R_m [MPa]	ε
as quenched	1		179	1
373	1		215	1
423	1		358	1
473	1		421	1
523	1		283	1
573	1	A	246	1
623	1		65	1
673	1	(S.R.)	51	1
698			43	1
723	1		7	0.008
773	1	A+αFe	*	*
823	1		*	*
873	1	(P.C.)	*	*
923	1	αFe,Fe_2B,	*	*
973	1	HfB_2,FeB,	*	*
1023	1	Fe_2Hf (S.C.)	*	*
A – amorphous phase, (S.R.) – structural relaxation				
(P.C.) – primary crystallization, (S.C.) – second crystallization				
* - because of high brittleness of ribbons annealed from 773 K tensile tests haven't been carried out				

Table 3.
Influence of heat treatment on phase composition and mechanical properties (R_m, ε) of amorphous $Fe_{84}Nb_7B_9$ alloy

Heat treatment parameters		Phase composition	Tensile strength	Plastic deformation
Temperature T_a [K]	Time [h]		R_m [MPa]	ε
as quenched	1		732	1
573	1		823	1
623	1	A	769	0.033
673	1		294	0.028
723	1	(S.R.)	238	0.013
773	1		106	0.007
823	1	$A^{1)}$+α-Fe	49	0.005
873	1	(P.C.)	43	0.003
923	1	α-Fe, FeB,	24	0.001
973	1	Fe_2B, Fe_2Nb (S.C.)	20	0
A – amorphous phase, (S.R.) – structural relaxation (P.C.) – primary crystallization, (S.C.) – second crystallization				

Further increase of annealing temperature from 623 K up to 1023 K involves the significant changes in phase composition of investigated alloy. The existence of Fe_2Hf, Fe_2B, FeB and HfB_2 phases together with αFe phase has been identified on X-ray diffraction pattern for ribbons annealed at temperature T_a=623 K (Table 1).

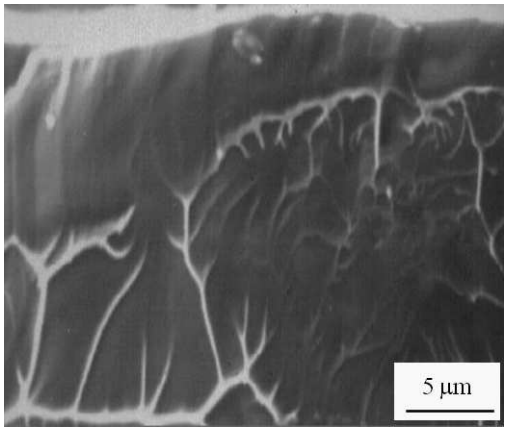

Fig. 5. SEM image of fracture surface of $Fe_{85.4}Hf_{1.4}B_{13.2}$ ribbons after decohesion in tensile test - annealing temperature 523K/1h; ductile vein pattern morphology

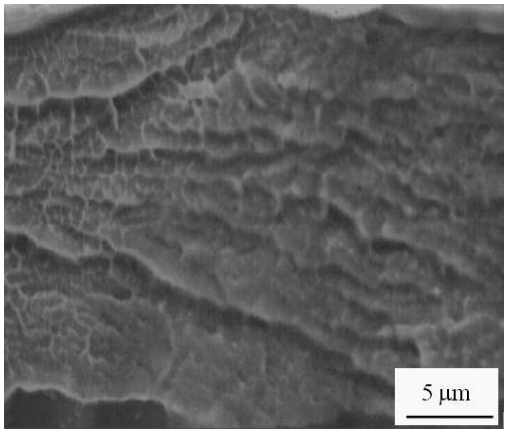

Fig. 6. SEM image of fracture surface of $Fe_{85.4}Hf_{1.4}B_{13.2}$ ribbons after decohesion in tensile test - annealing temperature 523K/1h; chevron pattern morphology

Starting with temperature annealing of 623 K total loss of plasticity and decrease of tensile strength R_m has been observed (Table 1). Together with the changes of mechanical properties of $Fe_{85.4}Hf_{1.4}B_{13.2}$ ribbons annealed in temperature range from 623 K up to 1023 K is corresponding the morphology of fracture after decohesion in tensile testing.

Well noticeable changes of the morphology fractures confirm the progress of the alloy crystallization process. The failure surface of $Fe_{85.4}Hf_{1.4}B_{13.2}$ ribbons annealed at 723 K and above had intercrystalline character (Fig. 9, 10).

The investigations of $Fe_{76.6}Hf_{6.4}B_{17}$ alloy showed that annealing at temperature to 698 K didn't bring fundamental changes of structure and plastic properties of the samples in compare to as quenched state (Table 2). Failure surface of ribbons after decohesion in tensile testing still showed their ductile

character of fracture with typical vein pattern morphology of dense veins network and partially shell type fracture (Fig. 11, 12). Tensile strength R_m is between 421 and 43 MPa (Table 2).

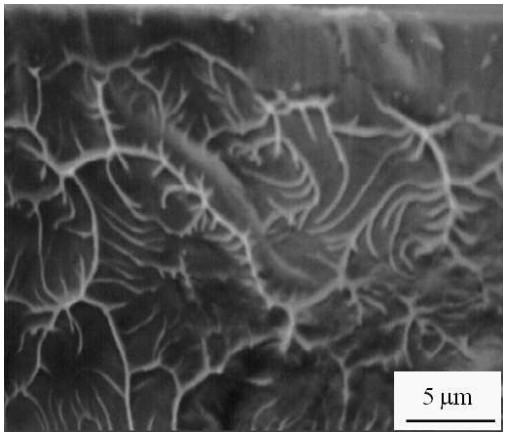

Fig. 7. SEM image of fracture surface of $Fe_{85.4}Hf_{1.4}B_{13.2}$ ribbons after decohesion in tensile test - annealing temperature 573K/1h; ductile vein pattern morphology

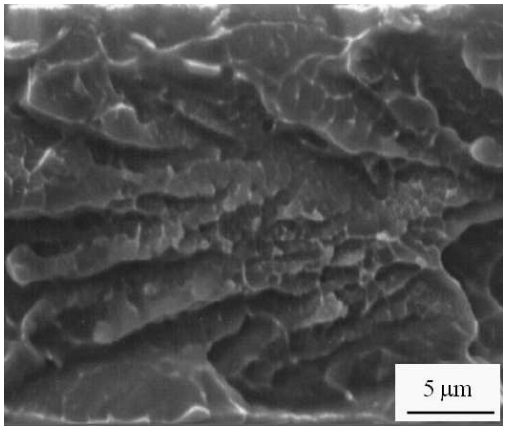

Fig. 8. SEM image of fracture surface of $Fe_{85.4}Hf_{1.4}B_{13.2}$ ribbons after decohesion in tensile test - annealing temperature 573K/1h; chevron pattern morphology

Further annealing of $Fe_{76,6}Hf_{6,4}B_{17}$ alloy in temperature range of 723 to 873 K is responsible for the crystallization of the amorphous matrix. The X-ray diffraction studies showed that the structure of the samples was formed by crystalline grains of αFe phase embedded in amorphous matrix (Table 2). After annealing at temperature 723 K ductility as well as tensile strength of the alloy have decreased respectively to ε=0.008 and R_m=7 MPa (Table 2). Because of high brittleness of the ribbons annealed from 773 K tensile tests haven't been carried out.

The observed decrease of mechanical properties is corresponding to partially smooth fracture surface (Fig. 13).

Increase of temperature annealing from 923 to 1023 involved further changes in phase composition of investigated alloy. Existance Fe_2Hf, Fe_2B, FeB and HfB_2 phases together with αFe phase has been identified on X-ray diffraction pattern (Table 2).

The significant changes observed in the fracture morphology of ribbons after decohesion are corresponding to the occurred structure changes. Morphology is changing from partially smooth character (Fig. 13) to intercrystalline fracture (Fig. 14).

Annealing of the $Fe_{84}Nb_7B_9$ alloy at temperature 573 K for 1 h didn't involve the changes of structure and plastic properties of the samples in compare to as quenched amorphous state (Table 3).

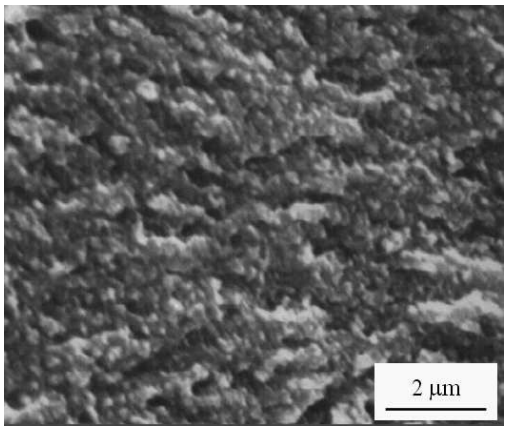

Fig. 9. SEM image of fracture surface of $Fe_{85.4}Hf_{1.4}B_{13.2}$ ribbons after decohesion in tensile test - annealing temperature 723K/1h; brittle fracture of intercrystalline character

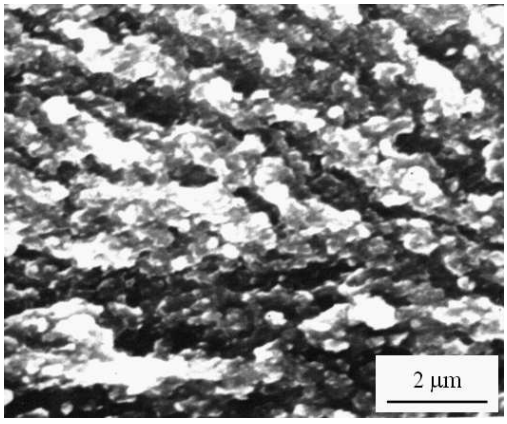

Fig. 10. SEM image of fracture surface of $Fe_{85.4}Hf_{1.4}B_{13.2}$ ribbons after decohesion in tensile test - annealing temperature 1023K/1h; brittle fracture of intercrystalline character

However, increase of tensile strength R_m up to value 823 MPa has been observed. So it can be stated that after annealing at temperature 573 K alloy reaches better tensile properties then in as quenched state, and plastic properties are still unchanged (ε=1). The fracture morphology of tapes after decohesion corresponds to characteristic ductile form with vein pattern but also with areas of chevron fracture morphology - Fig. 15. It's pointing out on the beginning of the structural relaxation process.

Increasing the temperature of annealing up to 623 K involves slight decrease of tensile strength, R_m=769 MPa but considerable loss of plastic properties of investigated ribbons is taking place.

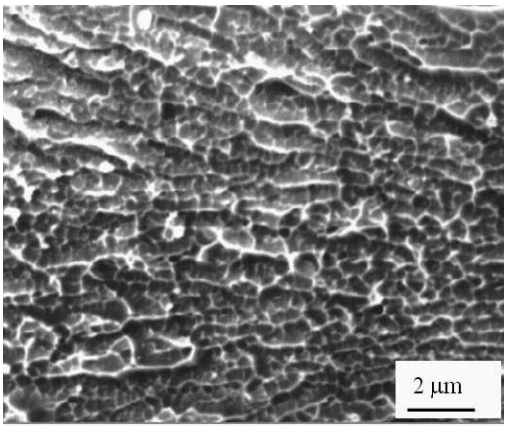

Fig. 11. SEM image of fracture surface of $Fe_{76,6}Hf_{6,4}B_{17}$ ribbons after decohesion in tensile test - annealing temperature 573K/1h; ductile fracture with dense veins network

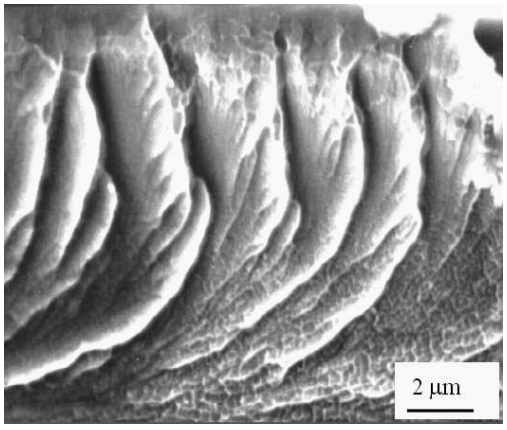

Fig. 12. SEM image of fracture surface of $Fe_{76,6}Hf_{6,4}B_{17}$ ribbons after decohesion in tensile test - annealing temperature 673K/1h; ductile shell fracture with dense veins network

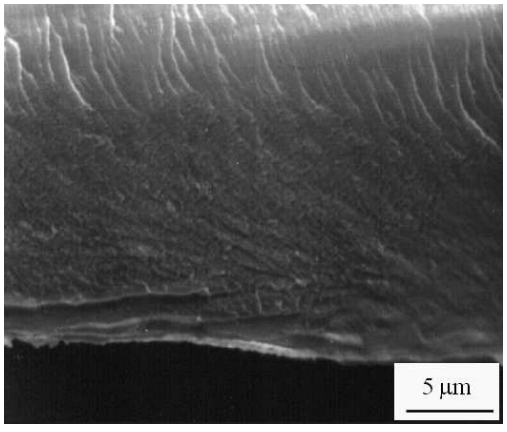

Fig. 13. SEM image of fracture surface of $Fe_{76,6}Hf_{6,4}B_{17}$ ribbons after decohesion in tensile test - annealing temperature 723K/1h; smooth fracture with partially shell areas

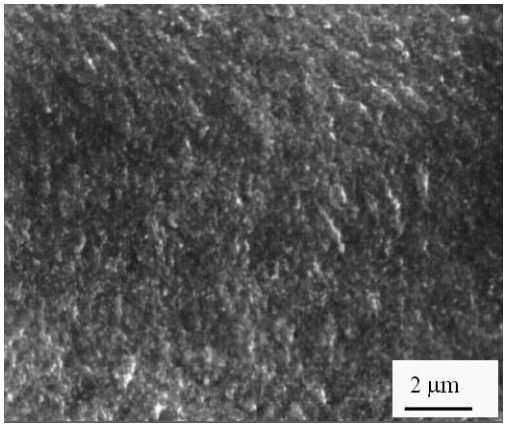

Fig. 14. SEM image of fracture surface of $Fe_{76,6}Hf_{6,4}B_{17}$ ribbons after decohesion in tensile test - annealing temperature 1023K/1h; brittle fracture of intercrystalline character

Ribbons are brittle and decrease of characteristic values describing plasticity is observed (ε=0.033), (Table 3). Fracture morphology observations confirmed the changes of plastic properties.

Characteristic chevron pattern morphology has been revealed on the fracture surface - Fig. 16.

Increase of the annealing temperature from 673-773 K leads to further loss of tensile strength, R_m=294-106 MPa, as well of plasticity (ε=0.028÷0,007), (Table 3).

Structure investigations showed that alloy has still amorphous structure in that temperature (Table 3). Fracture morphology is characteristic for chevron pattern (Fig. 17). That morphology points out on occuring the relaxation phenomena, which are conducting to considerable loss of high plasticity of investigated alloy.

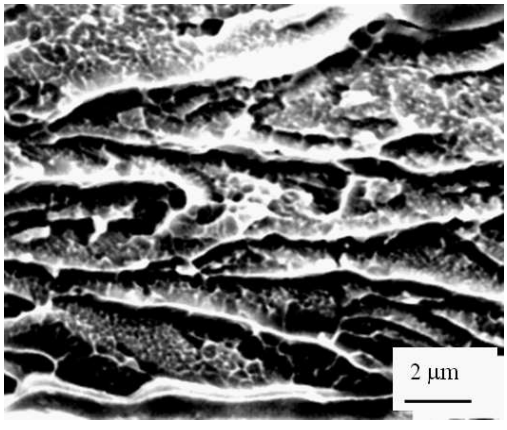

Fig. 15. SEM image of fracture surface of $Fe_{84}Nb_7B_9$ ribbons after decohesion in tensile test - annealing temperature 573 K/1h; ductile vein pattern morphology with areas of chevron fracture

Heat treatment process in annealing temperature range from 823 K up to 873 K involves the changes of the structures as well as the properties of investigated ribbons. Together with the temperature increase tensile strength R_m is decreasing from value of 49 MPa to 43 MPa. (Table 3).

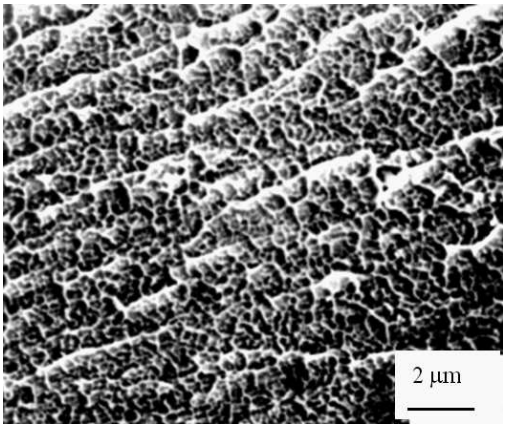

Fig. 16. SEM image of fracture surface of $Fe_{84}Nb_7B_9$ ribbons after decohesion in tensile test - annealing temperature 623 K/1h; chevron pattern morphology

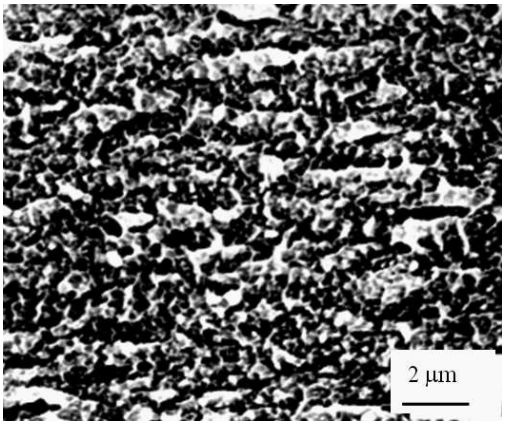

Fig. 17. SEM image of fracture surface of $Fe_{84}Nb_7B_9$ ribbons after decohesion in tensile test - annealing temperature 673 K/1h; chevron pattern morphology

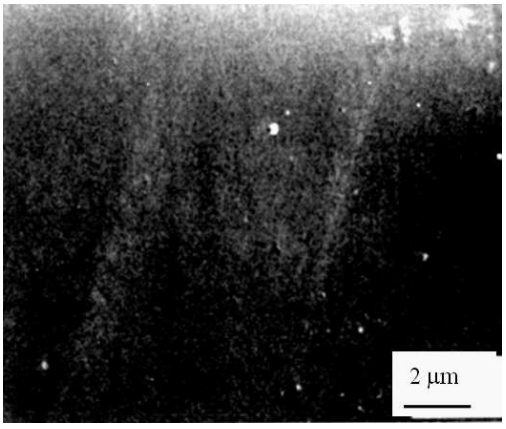

Fig. 18. SEM image of fracture surface of $Fe_{84}Nb_7B_9$ ribbons after decohesion in tensile test - annealing temperature 823 K/1h; smooth fracture

Loss of plastic properties of ribbons following the increase of annealing temperature has been observed. In the structure beside the amorphous phase, the α-Fe phase has been identified (Table 3). This phase is appearing in structure of ribbons annealed at temperature of 823 K.

Fractographic investigations of failure surfaces after decohesion in tensile test showed, in all ribbons annealed in temperature range 823 K to 873 K, the same morphology characterized by smooth fracture - Fig. 18.

Existance of FeB, Fe_2B and Fe_2Nb phases together with α-Fe phase has been identified on X-ray diffraction pattern for ribbons annealed at temperature over 923 K (Table 3).

The significant changes of fracture morphology of ribbons after decohesion are corresponding to the observed structure changes.

Morphology is changing from smooth character to intercrystalline fracture - Fig. 19. Annealing of specimens at temperature of 973 K by 1 hour doesn't involve further changes in phase composition of investigated alloy (Table 3). Fracture morphology of ribbons is characteristic for brittle crystalline materials and had still intercrystalline character.

4. Conclusions

The all investigated alloys had amorphous structure and good mechanical properties (R_m, ε=1) in as quenched state. Character of fracture morphology confirmed high plasticity of ribbons and revealed their ductile character with vein pattern morphology, typical for amorphous alloys.

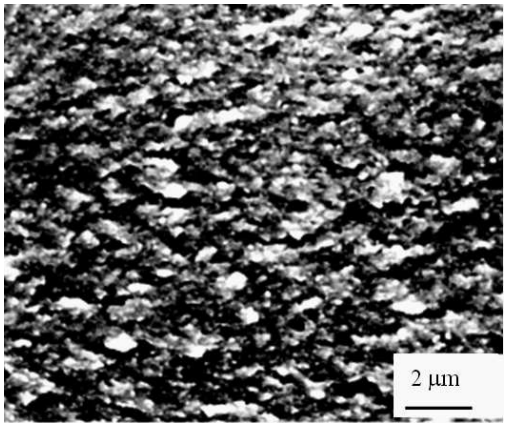

Fig. 19. SEM image of fracture surface of $Fe_{84}Nb_7B_9$ ribbons after decohesion in tensile test - annealing temperature 923 K/1h; brittle intercrystalline fracture

The carried out investigations have been showed that heat treatment of amorphous NANOPERM alloys involves structural relaxation and two-stage crystallization process what leads to radical changes of mechanical properties of ribbons. Depending on chemical alloy composition different temperature of first and second stage crystallization have been stated.

Heat treatment below temperature of crystallization accompanies structural relaxation of NANOPERM alloys. All alloys has still amorphous structure in that state.

As a result of primary crystallization in structure of ribbons annealed coexistence of amorphous phase and αFe phase has been stated.

The second stage of crystallization is characterized by simultanously crystallization of several phases identified as: Fe_2Hf, Fe_2B, FeB and HfB_2 phases together with αFe phase in Fe-Hf-B alloys and FeB, Fe_2B, Fe_2Nb both αFe phase in $Fe_{84}Nb_7B_9$ alloy. This stage of crystallization is responsible for the following loss of mechanical properties.

The character of the fracture morphology observed in ribbons after annealing in different temperatures ranges is corresponding to the changes of structure and mechanical properties for all investigated alloys.

Structural relaxation connected with annealing out of free volume frozen during rapid cooling as well as crystallization process of alloys confirm the observed fracture morphology with ductile vein pattern and chevron pattern.

The fracture morphology of the all alloys annealed in temperature range of primary crystallization have still vein and chevron pattern character.

Fracture morphology of ribbons annealed in temperature range of second crystallization have brittle intercrystalline character indicating high dispersion of structure obtained as a result of crystallization process of phases.

References

[1] E.E. Shalyguina, et al., Invertred near-surface hysteresis loop in annealed $Fe_{80.5}Nb_7B_{12.5}$ ribbons, Journal of Magnetism and Magnetic Materials 290-291 (2005) 1438-1441.

[2] E.E. Shalyguina, et al., Abnormal near-surface magnetic properties of heterogeneous (amorphous/nanocrystalline) $Fe_{80.5}Nb_7B_{12.5}$ ribbons, Thin Solid Films 505 (2006) 161-164.

[3] T. Kulik, Magnetically soft nanocrystalline materials obtained by the crystallization of metallic glasses, edited by Warsaw Univesity Press, Warszawa 1998 (in Polish).

[4] T. Kulik, et al., Temperature of nanocrystallisation of magnetically soft alloys for high-temperature applications, Journal of Materials Processing Technology 162-163 (2005) 215-219.

[5] W. Lu, et al., Nanocrystalline $Fe_{84}Nb_7B_9$ alloys prepared by mechanical alloying and ultra-high-pressure consolidation, Journal of Alloys and Compounds 413 (2006) 85-89.

[6] J. Konieczny, L.A. Dobrzański, J.E. Frąckowiak, Structure and megnetic properties of powder HITPERM material, Archives of Materials Science and Engineering 28/3 (2007) 156-163.

[7] S.H. Yoon, et al., Distributions of hyperfine parameters in nanocrystalline $Fe_{83}B_9Nb_7Cu_1$ alloys, Journal of Magnetism and Magnetic Materials 254-255 (2003) 507-509.

[8] J. Tang, X. Mao, S. Li, W. Gao, Y. Du, Effects of two-step annealing on the microstructures and soft magnetic properties of nanocrystalline $Fe_{86}Zr_7B_6Cu_1$ ribbons, Journal of Alloys and Compounds 375 (2004) 233-238.

[9] D. Szewieczek, J. Tyrlik-Held, S. Lesz, Structure and mechanical properties of amorphous $Fe_{84}Nb_7B_9$ alloy during crystallization, Journal of Achievements in Materials and Manufacturing Engineering 24/2 (2007) 87-90.

[10] D. Szewieczek, J. Tyrlik-Held, S. Lesz, Influence of crystallization of amorphous $Fe_{84}Nb_7B_9$ alloy on the structure, mechanical properties and fracture morphology after decohesion, Proceedings of the 8th International Scientific Conference „Achievements in Mechanical and Materials Engineering" AMME'99, Gliwice-Rydzyna- Pawłowice-Rokosowo, 1999, 575-580 (in Polish).

[11] S. Lesz, D. Szewieczek, J.E. Frąckowiak, Evolution of structure and magnetic proporties of amorphous $Fe_{85.4}Hf_{1.4}B_{13.2}$ alloy obtained by controlled crystallization, Journal of Achievements in Materials and Manufacturing Engineering 19/2 (2006) 29-34.

[12] D. Szewieczek, J. Tyrlik-Held, S. Lesz, Changes of mechanical properties and fracture morphology of amorphous tapes involved by heat treatment, Journal of Materials Processing Technology 109 (2001) 190-195.

[13] H. Chiriac, C. Hinson, Mechanical behaviour of nanocrystalline Fe-Hf-B ribbons, Journal of Magnetism and Magnetic Materials 254-255 (2003) 475-476.

[14] P. Kwapuliński, et al., Magnetic properties of amorphous and nanocrystalline alloys based on iron, Journal of Materials Processing Technology 157-158 (2004) 735-742.

[15] D. Szewieczek, T. Raszka, J. Olszewski, Optimisation the magnetic properties of the $(Fe_{1-x}Co_x)_{73.5}Cu_1Nb_3Si_{13.5}B_9$ (x=10,30,40) alloy, Journal of Achievements in Materials and Manufacturing Engineering 20 (2007) 31-36.